THE JOURNAL OF BIOLOGICAL CHEMISTRY
Vol. 273, No. 50, Issue of December 11, pp. 33386–33396, 1998

Printed in U.S.A.

DnaB Helicase Is Unable to Dissociate RNA-DNA Hybrids

ITS IMPLICATION IN THE POLAR PAUSING OF REPLICATION FORKS AT ColE1 ORIGINS*

(Received for publication, June 30, 1998, and in revised form, September 28, 1998)

David Santamaría‡, Guillermo de la Cueva§, María Luisa Martínez-Robles‡, Dora B. Krimer‡, Pablo Hernández‡, and Jorge B. Schvartzman‡¶

From the ‡Departamento de Biología Celular y del Desarrollo and §Departamento de Microbiología Molecular, CIB (Consejo Superior de Investigaciones Científicas), Velázquez 144, 28006 Madrid, Spain

A series of plasmids were constructed containing two unidirectional ColE1 replication origins in either the same or opposite orientations and their replication mode was investigated using two-dimensional agarose gel electrophoresis. The results obtained showed that, in these plasmids, initiation of DNA replication occurred at only one of the two potential origins per replication round regardless of origins orientation. In those plasmids with inversely oriented origins, the silent origin act as a polar pausing site for the replication fork initiated at the other origin. The distance between origins (up to 5.8 kilobase pairs) affected neither the interference between them to initiate replication nor the pausing function of the silent origin. A deletion analysis indicated that the presence of a transcription promoter upstream of the origin was the only essential requirement for it to initiate replication as well as to account for its polar pausing function. Finally, *in vitro* helicase assays showed that *Escherichia coli* DnaB is able to melt DNA-DNA homoduplexes but is very inefficient to unwind RNA-DNA hybrids. Altogether, these observations strongly suggest that replication forks pause at silent ColE1 origins due to the inability of DnaB helicase, which leads the replication fork *in vivo*, to unwind RNA-DNA hybrids.

The difficulty to generate palindromes involving ColE1 origins is a well known paradox (1, 2). Indeed, co-orientation of replication origins is the most common organization found in nature for multimeric plasmids. *Streptococcus pyogens* broad host range plasmid pSM19035 is one of the few exceptions (3, 4). pPI21, an *Escherichia coli* plasmid derivative of pSM19035 and pBR322, has two long inverted repeats, each one containing a potentially active ColE1 unidirectional origin. It was recently shown that progression of the replication fork initiated at either of the two potential origins of pPI21 is transiently stalled at the other inversely oriented origin (5). This pausing leads to the accumulation of a specific replication intermediate (RI)[1] containing an internal bubble that spans the distance between both origins. The accumulated RI exists as a series of stereoisomers that may have one or more knots with a different number of nodes within the replicated portion (5). Whether this peculiar replication behavior is specific for *S. pyogens* pSM19035-derived plasmids or a general feature for all plasmids containing two inversely oriented ColE1 origins is still to be shown. Moreover, nothing is known about the mechanism responsible for the transient pausing of replication forks as they encounter another silent and inversely oriented ColE1 origin; and the palindromic structure of pPI21 made it difficult to find out whether or not both origins were equally competent to initiate DNA replication.

To answer all these questions, we constructed a series of *E. coli* plasmids containing two unidirectional ColE1 origins in either the same or opposite orientations. Two-dimensional agarose gel electrophoresis (6) was then used to study the replication mode of these plasmids in order to investigate the interference between the origins and the efficiency of complete or partially deleted origins to initiate replication as well as to stall replication forks initiated at the other origin. We hoped these experiments would shed new light on the mechanism responsible for the polar pausing of replication forks at other silent and inversely oriented ColE1 origins. In this way they would help us to understand why palindromes involving ColE1 origins are so rare in nature and even difficult to obtain in the laboratory.

EXPERIMENTAL PROCEDURES

Bacterial Strains and Culture Medium—The *E. coli* strain used in this study was DH5αF′. Competent cells were transformed with monomeric forms of the plasmids as described elsewhere (7). Cells were grown at 37 °C in LB medium containing 50 μg/ml ampicillin unless otherwise specified.

Plasmid Constructions—To construct pHH0.5 and pHT0.5, the 759-bp-long *Afl*III-*Dra*I fragment from pUC19 was blunt-ended with Klenow and cloned in both orientations into the *Sma*I site of pUC19 dephosphorylated with CIP. pHH2.0 and pHT2.0 were obtained by digesting pHH0.5 and pHT0.5 between the origins with *Hin*cII and CIP dephosphorylated. The 1,453-bp-long *Eco*RI fragment from YRp7′ containing the ARS1-trp cassette was blunt-ended with Klenow and cloned into *Hin*cII-cleaved pHH0.5 and pHT0.5. pHH5.8 and pHT5.8 were obtained by cutting pHH2.0 and pHT2.0 between the origins with *Eco*RV and CIP dephosphorylated. A 3,851-bp-long *Eco*RI-*Kpn*I fragment from human rDNA was blunt-ended with T4 polymerase and cloned into *Eco*RV-cleaved pHH2.0 and pHT2.0.

To construct pHH/BR-BR2.9, the 1,165-bp-long *Pvu*II-*Dra*I fragment from pBR322 containing the complete ColE1 origin was cloned into *Eco*RV-cleaved pBR322 dephosphorylated with CIP. pHH/BR-ΔRNAS2.9 was constructed inserting the 820-bp-long *Alw*NI-*Pvu*II fragment from pBR322 into *Eco*RV-cleaved pBR322 that was previously made blunt-ended with T4 polymerase. To construct pHH/BR-Δpass2.9, the 759-bp-long *Dra*I-*Afl*III fragment from pBR322 was blunt-ended with Klenow and cloned into *Eco*RV-cleaved pBR322. Finally, pHH/

* This work was supported in part by Grant 96/0470 from the Spanish Fondo de Investigación Sanitaria, Grant PM95/0016 from the Spanish Dirección General de Enseñanza Superior, Grant 08.6/0016/1997 from the Comunidad de Madrid, and Grant PB94–0127 from the Spanish Comisión Interministerial de Ciencia y Tecnología. The costs of publication of this article were defrayed in part by the payment of page charges. This article must therefore be hereby marked "*advertisement*" in accordance with 18 U.S.C. Section 1734 solely to indicate this fact.

¶ To whom correspondence should be addressed: Dept. de Biología Celular y del Desarrollo, CIB-CSIC, Velázquez 144, 28006 Madrid, Spain. Tel.: 34-91-564-4562 (ext. 4233) or 34-91-561-1800 (ext. 4233); Fax: 34-91-564-8749; E-mail: cibjb21@fresno.csic.es.

[1] The abbreviations used are: RI, replication intermediate; bp, base pair(s); kb, kilobase pair(s); pol, polymerase; CIP, calf intestinal phosphatase; OC, open circle.

BR18-ΔRNAs2.9 was constructed cutting pHH/BR-ΔRNAs with *Eco*RI and *Hin*dIII to eliminate the tetracycline promoter, and this fragment was replaced with a 51-bp *Eco*RI-*Hin*dIII fragment from pUC19 containing the multiple cloning site.

Isolation of Plasmid DNA—Cells from overnight cultures were diluted 40-fold into fresh LB medium, grown at 37 °C to exponential phase (A_{600} = 0.4–0.6), quickly chilled, and centrifuged. 1000 ml of cultured cells were washed with 20 ml of STE buffer (0.1 M NaCl, 10 mM Tris-HCl, pH 8.0, and 1 mM EDTA, pH 8.0), harvested by centrifugation, and resuspended in 5 ml of 25% sucrose and 0.25 M Tris-HCl, pH 8.0. Lysozyme (10 mg/ml) and RNase A (0.1 mg/ml) were added, and the suspension was maintained on ice for 5 min. Afterward, 2 ml of 0.25 M EDTA, pH 8.0, were added, and the suspension was kept on ice for another 5 min. Cell lysis was achieved by adding 8 ml of lysis buffer (1% Brij-58, 0.4% sodium deoxycholate, 0.063 M EDTA, pH 8.0, and 50 mM Tris-HCl, pH 8.0) and keeping the lysate for 15 min on ice. The lysate was centrifuged at 26,000 × *g* for 45 min at 4 °C to pellet the chromosomal DNA and other bacterial debris. Plasmid DNA was recovered from the supernatant and precipitated by adding 2/3 volume of 25% polyethylene glycol 6000 and 1.25 M NaCl in TE (10 mM Tris-HCl, pH 8.0, and 1 mM EDTA) and kept overnight at 4 °C on ice. The precipitated DNA was pelleted by centrifugation at 6,000 × *g* for 15 min at 4 °C and the pellet resuspended and incubated in 5 ml of a preheated digestion buffer (100 μg/ml proteinase K in 1 M NaCl, 10 mM Tris-HCl, pH 9.0, 1 mM EDTA, and 0.1% SDS), at 37 °C for 60 min. Proteins were extracted twice with phenol:chloroform:isoamyl alcohol (25:24:1) equilibrated with 10 mM Tris-HCl, pH 8.0, and then extracted once with chloroform: isoamyl alcohol (24:1). The DNA was precipitated with 2.5 volumes of absolute ethanol overnight at −20 °C and resuspended in TE. The DNA was digested with restriction endonucleases (Boehringer Mannheim) as recommended by the manufacturer in the presence of 100 μg/ml RNase A.

Two-dimensional Agarose Gel Electrophoresis—Analysis of RIs by two-dimensional agarose gel electrophoresis was performed as described elsewhere (7). The first dimension was in a 0.28–0.4% agarose gel in TBE buffer at 1 V/cm and room temperature for 22–38 h. The lane containing the λ DNA-*Hin*dIII marker sizes was excised, stained with 0.5 μg/ml ethidium bromide, and photographed. In the meantime, the lanes containing DNA RIs were kept in the dark. The second dimension was in a 0.85–1% agarose gel in TBE containing 0.3 μg/ml ethidium bromide at a 90° angle with respect to the first dimension. The dissolved agarose was poured around the excised lane from the first dimension, and electrophoresis was at 5 V/cm in a 4 °C cold room for 6–8 h.

Southern Transfer and Hybridization—Gels were washed for 15 min in 0.25 N HCl before an overnight transfer to Zeta-Probe blotting membranes (Bio-Rad) in 0.4 N NaOH. Prehybridization was carried out in 2× SSPE (3.6 M NaCl, 0.2 M Na_2HPO_4, 20 mM EDTA), 1% SDS, 10% dextran sulfate, 0.5% Blotto, and 250 mg/ml sonicated salmon sperm DNA at 65 °C. After 4 h, 6 × 10^5 cpm/ml of probe DNA labeled with [^{32}P]dCTP by random priming was added and incubated at 65 °C overnight. After hybridization the membranes were washed in 2% SSC, 0.1% SDS at room temperature for 15 min, followed by an additional 15 min in 0.5% SSC, 0.1% SDS also at room temperature. The last 15-min wash was in 0.1% SSC, 0.1% SDS at 65 °C. Exposure of Curix RP2 (Agfa) films was carried out at −80 °C with two intensifying screens for 1–3 days.

Purification of DnaB Protein—DnaB of *E. coli* was purified following a modification of the procedure developed by (8). Three liters of BL21(DE3) cells transformed with the DnaB overproducer (pET11b-DnaB) were induced with isopropyl-1-thio-β-D-galactopyranoside, and a soluble fraction was obtained breaking the cells with liquid nitrogen and lysozyme (0.2 mg/ml) in lysis buffer (50 mM Tris-HCl, pH 8.0, 25 mM NaCl, 10 mM β-mercaptoethanol, 10 mM $MgCl_2$, 0.1 mM ATP, and 10% glycerol). DnaB was then precipitated with 0.2 g/ml ammonium sulfate, resuspended, and dialyzed against buffer A (50 mM Tris-HCl, pH 7.5, 25 mM NaCl, 10 mM β-mercaptoethanol, 10 mM $MgCl_2$, 0.1 mM ATPm and 10% glycerol. The dialyzed fraction was loaded onto a DEAE-Sephacel column equilibrated with buffer A, and a gradient between buffers A and B (the same as buffer A but with 800 mM NaCl) was run. The DnaB fractions obtained were then pooled, dialyzed against buffer A, and loaded onto a 5-ml Q-Sepharose Hi-Trap prepackaged column (Pharmacia). A salt gradient was run between buffers A and B. DnaB fractions were then pooled and stored at −70 °C in the presence of 50% glycerol. DnaB concentration was determined with a spectrophotometer at 280 nm.

Preparation of Helicase Substrates—The DNA-DNA helicase substrate was prepared phosphorylating 10 pmol of the oligonucleotide: 5′-CAGTCACGACGTTGTAAAACGACGGCCAGTCTTAAAAAAAAAA-AA-3′ with T4 polynucleotide kinase (Pharmacia) and [γ-^{32}P]ATP (ICN) in 50 μl of total volume. The phosphorylated oligonucleotide was purified through G-25 Sepharose, annealed to 1 pmol of pBlueScript KS+ single-stranded DNA in 100 μl of total volume and purified again through a CL-4B column.

The RNA-DNA helicase substrate was obtained by an *in vitro* transcription reaction of *Hin*dIII-cleaved pBlueScript KS+. The transcription reaction mixture (20 μl) contained 40 mM Tris-HCl, pH 8.0; 6 mM $MgCl_2$; 10 mM dithiothreitol; 2 mM spermidine; 500 μM each of ATP, CTP, and GTP; 100 μCi of [α-^{32}P]UTP 800 Ci/mmol (Amersham); 20 units of RNase inhibitor (Boehringer Mannheim); 10 units of T7 RNA polymerase (Boehringer Mannheim); and 500 ng of DNA template. The mixture was incubated at 37 °C for 45 min. Ten units of RQ1 DNase (Boehringer Mannheim) were added, and the mixture was incubated for an additional 15 min. The volume was increased to 100 μl with diethylpyrocarbonate-treated water and extracted with an equal volume of phenol:chloroform:isoamyl alcohol (25:24:1).

Helicase Assays—A standard reaction mixture (in a total volume of 20 μl) for DnaB and helicase II contained 10 fmol of the specific substrate employed (DNA-DNA or RNA-DNA) in 50 mM Tris-HCl, pH 7.5, 4 mM $MgCl_2$, 2 mM ATP, 50 mM potassium glutamate, 50 mg/ml bovine serum albumin, and 5 mM dithiothreitol (9). Indicated amounts of DnaB or helicase II were added to the substrate and incubated for 10 min (helicase II) or 30 min (DnaB) at 37 °C. Reactions were terminated by addition of a dye mixture containing SDS-EDTA-sucrose and bromphenol blue. The end products were analyzed by electrophoresis through a 3–10% polyacrylamide gel in Tris borate-EDTA buffer. Exposure of Curix RP2 (Agfa) films to the dried gels was carried out at −80 °C with two intensifying screens for 1–12 h. The percentage of oligonucleotide released from the substrate was determined using a PhosphorImager densitometer.

RESULTS

One of our primary goals was to find out whether or not the polar pausing of a replication fork at another origin was a general feature for all plasmids containing two inversely oriented ColE1 origins. We wanted to answer this question using two-dimensional gels to study the RIs of non-palindromic plasmids to determine if both origins were equally competent to initiate replication. Finally, we also wanted to know if the physical distance between the origins affected their capacity to interfere with each other and to act as a replication pausing site.

Two series of plasmids were constructed containing two potentially active ColE1 origins either in the same or in opposite orientations. Each series comprised three different plasmids, where the distance between origins was approximately 0.5, 2.0, and 5.8 kb, respectively (Fig. 1). A small fragment of pUC19 containing the ColE1 origin was inserted into the *Sma*I site of this same vector, in both orientations. We previously confirmed that the aforementioned DNA fragment was able to confer autonomous replication to plasmids lacking a replication origin (data not shown). In this way we obtained the first two plasmids of each series: pHH0.5 and pHT0.5. HH points to the head-to-head orientation, while HT indicates head-to-tail orientation. 0.5 refers to the distance between the origins (in kb). Next, pHH2.0 and pHT2.0 were constructed where the distance between origins had increased from 0.5 to 2.0 kb. Finally, we built up pHH5.8 and pHT5.8, the third member of each series, where the distance between origins was approximately 5.8 kb. Fig. 1 shows the restriction maps and the construction sequence followed to make the pHH series. As indicated before, the pHT series was constructed in a similar fashion (for details, see "Experimental Procedures").

We used a computer program (10) to predict the shape of the RIs as well as the two-dimensional agarose gel patterns expected for each of the experiments performed throughout this study. To illustrate its usefulness, Fig. 2 shows the predictions made by the program for the RIs corresponding to pHH2.0 after digestion with *Kpn*I. Two series of RIs were drawn by the program depending on whether initiation occurs only at the

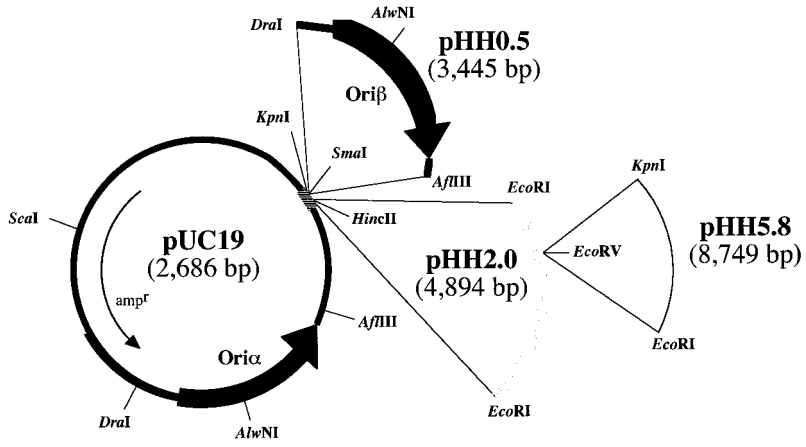

FIG. 1. **Construction strategy and restriction map of the plasmids derived from pUC19 containing two ColE1 origins.** Only the pHH series is presented in the figure. A similar strategy was used to construct the pHT series (for details, see text). The restriction map to the *left* corresponds to the circular plasmid pUC19. The *thick arrow* on the *circle* indicates the location and orientation of the complete origin (Oriα). The *thin arrow* within the *circle* indicates the location and transcription direction of the ampicillin resistance gene. The *hatched zone* marks the polycloning site. The places for a number of restriction endonucleases with a single recognition site are indicated. The *thick arrow* outside the pUC19 map represents the *Dra*I-*Afl*III minimal origin (Oriβ) that was cloned into the *Sma*I site of pUC19 to generate pHH0.5. The *thick stippled* arc below corresponds to an *Eco*RI fragment from *S. cerevisiae* that was cloned into the *Hin*cII site of pHH0.5 to generate pHH2.0. Finally, the *thin black arc* at the *far right* corresponds to a *Kpn*I-*Eco*RI fragment from human rDNA that was cloned into the *Eco*RV site of pHH2.0 to generate pHH5.8. The names of the resulting plasmids and their sizes (in bp) are indicated.

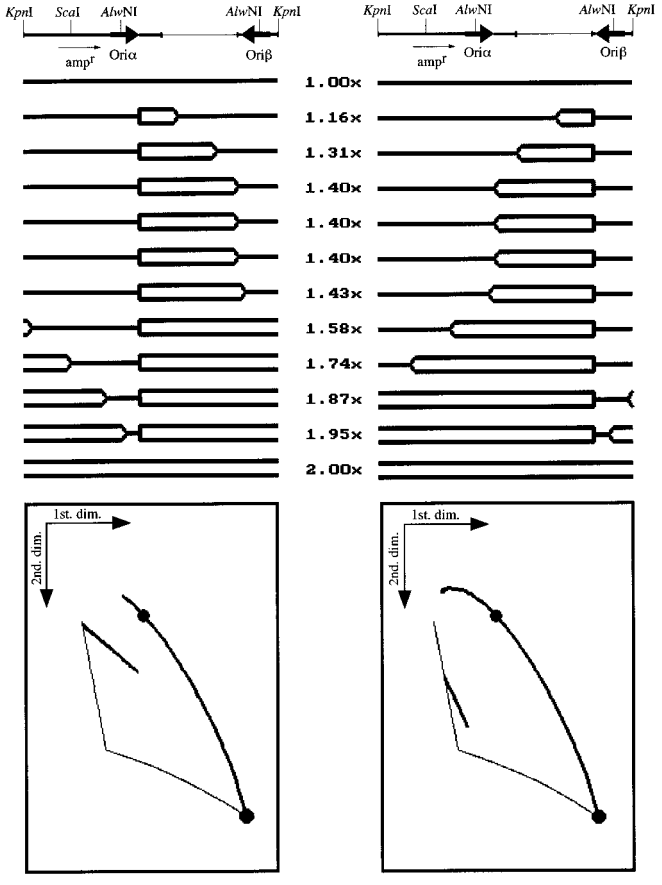

FIG. 2. **The mass and shape of some RIs and the corresponding two-dimensional gel patterns expected for pHH2.0 digested with *Kpn*I are shown as diagrammed by the computer.** Linear maps are shown at the *top*. To the *left*, the RIs and the pattern expected if initiation only occurs at Oriα. To the *right*, the RIs and the pattern expected if initiation only occurs at Oriβ.

native origin, hereafter defined as oriα (shown to the *left*), or only at the new origin, named oriβ (shown to the *right*). If initiation only occurs at oriα, a bubble would be formed that would grow rightward until the replication fork reaches the right end of the fragment. At this point the molecular mass of the RI would be 1.54× the mass of the linear unreplicated form (between 1.43 and 1.58). When the replication fork reaches the right end of the fragment, the bubble would open up and the shape of the RIs would change abruptly from a bubble to a simple-Y. As the replication fork leaves the fragment by the right end, it re-enters by the left end still moving rightward, and the shape of the RIs changes again from a simple to a double-Y. If initiation only occurs at oriβ, the shape of the RIs would be similar, although in this case the replicating fork would progress leftward. More importantly, when the bubble opens up as the replication fork reaches the left end of the fragment, the mass of the RI would be 1.85× (between 1.74 and 1.87) instead of 1.54×, as in the previous case. If the replication fork initiated at one origin pauses as it encounters the other silent origin, a specific RI would accumulate in both cases with a relative mass of approximately 1.4×. The predicted two-dimensional agarose gel pattern corresponding to each series of RIs are shown in the *lower part* of Fig. 2. As indicated earlier, a similar prediction was made for all the plasmids analyzed throughout this study before the two-dimensional agarose gel experiments were actually performed.

Interference between Origins and Polar Pausing of the Replication Fork at the Silent Origin Are General Features for All Plasmids Bearing Two Inversely Oriented ColE1 Origins—Plasmid DNA was isolated from exponentially growing cells that had been transfected with each of the six previously described plasmids. pHH0.5 and pHT0.5 DNAs were digested with *Sca*I, pHH2.0 and pHT2.0 were digested with *Kpn*I, and pHH5.8 and pHT5.8 were digested with *Alw*NI. Finally, the RIs of all six plasmids were independently analyzed by two-dimensional agarose gel electrophoresis (6). Fig. 3 shows the autoradiograms corresponding to pHH0.5, pHH2.0, pHT2.0, and pHH5.8. pHH0.5 was hybridized with the entire pUC19 DNA, used as a probe. pHH2.0 and pHT2.0 were hybridized with the entire pHH0.5 DNA. Finally, pHH5.8 was hybridized with the 3,851-bp *Eco*RI-*Kpn*I fragment from human rDNA. As in all these cases, initiation of DNA replication could occur at either the native (oriα) or the new (oriβ) origin; the patterns observed in the autoradiograms were expected to be a mixture of both populations. In Fig. 3*A*, corresponding to pHH2.0 digested with *Kpn*I (see Figs. 1 and 2), the *lower diagonal arc*

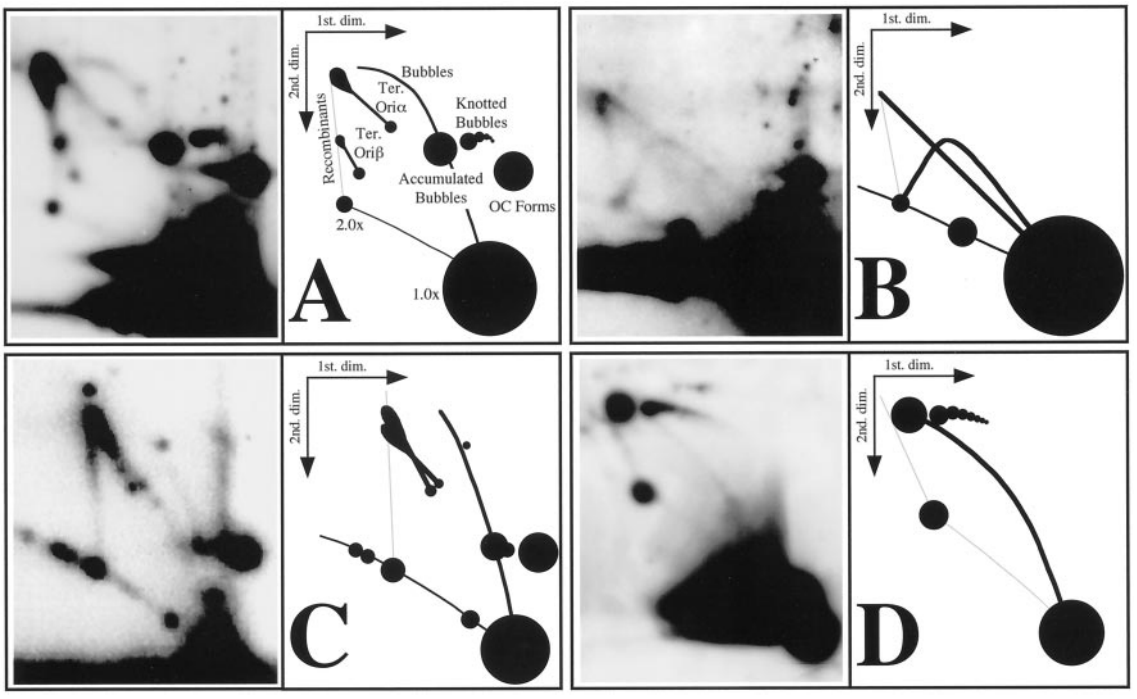

FIG. 3. **Two-dimensional agarose gel electrophoresis of the RIs corresponding to four different plasmids.** *A*, pHH2.0 linearized with *Kpn*I; *B*, pHT2.0 digested with *Kpn*I; *C*, pHH0.5 linearized with *Sca*I; *D*, the *Alw*NI fragment of pHH5.8 containing both origins. The photographs of selected autoradiograms are shown to the *left* with a diagrammatic interpretation to the *right*. These diagrams were prepared after studying different exposures in order to confirm the nature of each signal. The names given throughout the text to the most prominent signals are depicted only for pHH2.0 digested with *Kpn*I (*A*).

corresponded to linear forms (6, 7, 11, 12). The prominent spot at the *far right end* of the linear forms corresponded to the unreplicated linear form of the plasmid (1.0×). The other spot on the linear forms, to the *left*, corresponded to partial digestion of dimeric forms (2.0×). The prominent spot above the 1.0× linear form to the *right* was probably due to OC forms. The continuous signal extending upward from the 1.0× linear form to the upper part of the autoradiogram corresponded to a bubble arc. A discrete spot was observed on top of the bubble arc to the left of the OC forms. This spot was due to accumulated bubbles (5). A small arc formed by a series of spots with decreasing intensity was observed between the accumulated bubbles and the OC forms. This series of spots corresponded to knotted bubbles (5). Another faint and continuous arc occurred just underneath the bubble arc (only visible in very long exposed autoradiograms). This faint arc corresponded to simple-Ys and was probably due to the RIs of multimeric forms of the plasmid (6, 7, 11–14). Two discrete spots were clearly visible on the faint simple-Y arc. The relative mass of the molecules responsible for the smaller of these spots was slightly bigger than 1.5× as it occurred just to the left of the inflection point of the simple-Y arc. The other spot was due to molecules with a relative mass between 1.5 and 2.0×. A double-Y signal emerged from each one of these spots and extended upward and tilted to the left toward the signal corresponding to X-shaped recombinants. The intensity of both signals was very similar, and they became progressively stronger as they got closer to the X-shaped recombinants.

Fig. 3*B* shows the autoradiogram corresponding to pHT2.0 digested with *Kpn*I. In this plasmid, both origins were co-oriented. The patterns observed were completely different from those corresponding to pHH2.0 digested with the same restriction enzyme (Fig. 3*A*). No signal indicative for accumulated bubbles or knotted bubbles were detected.

Altogether, these results demonstrated that two-dimensional gels can be effectively used to monitor the efficiency of each origin to initiate replication by estimating the relative intensity of the double-Y signals corresponding to each origin. They also showed that initiation occurred at only one origin per replication round. The detection of accumulated bubbles and knotted bubbles in all the plasmids of the pHH series demonstrated that the peculiar replication behavior originally described for pPI21 was not specific for *S. pyogens* pSM19035-derived plasmids but a general feature for all plasmids containing two inversely oriented ColE1 origins. Finally, the differences observed between the pHH and pHT series demonstrated that stalling of the replication fork at the other silent origin was polar since it only happened if both origins were in opposite orientations.

The Distance between Origins (Up to 5.8 kb) Affected Neither the Interference between Them to Initiate Replication Nor the Pausing Function of the Silent Origin—Fig. 3*C* shows the autoradiogram corresponding to pHH0.5 digested with *Sca*I. The accumulated bubbles and two different termination signals were clearly distinguished. In this case the accumulated bubble had a relative mass of 1.15×. For this reason and due to its proximity to the prominent spot generated by OC forms, knotted bubbles were not clearly identified in the autoradiogram. In this particular plasmid, the termination signal for oriα started on the simple-Y arc with a relative mass of 1.53×, whereas the termination signal for oriβ started with a relative mass of 1.61×. Despite their proximity, both signals were clearly distinguished.

Fig. 3*D* shows the autoradiogram corresponding to pHH5.8 DNA digested with *Alw*NI. In this particular case, the accumulated bubbles had a relative mass of 1.89×. The prominent spot generated by these accumulated bubbles and the small arc formed by a series of spots with decreasing intensity, corresponding to knotted bubbles, were clearly identified. Since the fragment analyzed was palindromic (see Fig. 1), the termination signals corresponding to initiation of DNA replication at oriα and oriβ co-migrated in this autoradiogram.

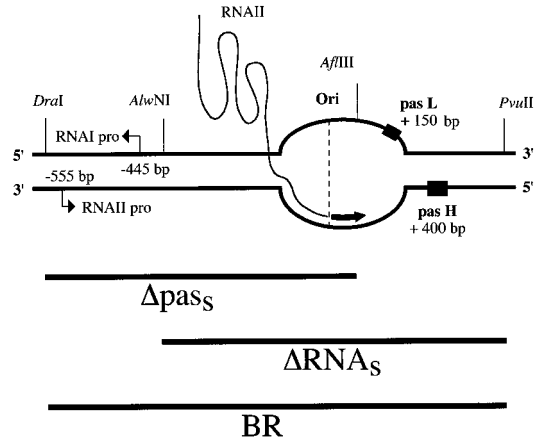

FIG. 4. **Diagram corresponding to the structure of a ColE1 origin (modified from Kornberg and Baker (Ref. 39)).** The recognition sites for several restriction endonucleases are depicted as well as the locations of the RNAI and RNAII promoters, pasL and pasH, with respect to Ori. The DNA restriction fragments containing the complete origin (*BR*) and the partially deleted ones (Δ*pass* and Δ*RNAs*) are indicated.

Detection of the signals corresponding to accumulated bubbles and knotted bubbles in all three plasmids containing inversely oriented origins indicated that the distance between them (up to 5.8 kb) affected neither their capacity to interfere with each other nor their ability to act as a replication pausing site.

Partially Deleted Origins Are Less Efficient Than a Complete Origin to Initiate Replication—Fig. 4 highlights some structural elements and the most important events going on at ColE1 origins as initiation of DNA replication progresses (15–20).

The ColE1 replication origin of the pUC vectors, oriα in our pHH and pHT series, has the *lacZ* gene with the polylinker inserted between pasH and pasL; the minimal origin we used as oriβ lacked both pasH as well as pasL. Nevertheless, both origins initiated replication quite efficiently (see Fig. 3). We ignored, however, whether or not these partially modified origins were as competent as a *bona fide* origin to initiate replication.

To find out more about the role of the pas sites and the promoters for RNAI and II in the competence of ColE1 origins to initiate replication and to act as a pausing site, we constructed three new plasmids: pHH/BR-BR2.9, pHH/BR-Δpass2.9, and pHH/BR-ΔRNAs2.9. HH refers to the head-to-head configuration of the origins. The following first BR indicates that Oriα is a complete origin. Next, the nature of Oriβ is indicated; it could be either BR (a complete origin), Δpass (where pasL and pasH were deleted), or ΔRNAs (where the promoters for RNAI and RNAII were deleted). Finally, 2.9 indicates that both origins are 2.9 kb apart. To build up the first of these plasmids, the 1,166-bp *Dra*I/*Pvu*II fragment of pBR322, containing both promoters as well as both pas sites (see Fig. 4), was inserted into the *Eco*RV restriction site of this same vector. In this way we obtained a plasmid containing two complete ColE1 origins in opposite orientations. pHH/BR-Δpass2.9 was constructed by inserting the 759-bp *Dra*I/*Afl*III fragment from pBR322 into the *Eco*RV site of this same vector. In this way we obtained a plasmid containing one complete origin and another origin lacking the pas sites, in opposite orientations (see Figs. 4 and 5). Finally, the 823-bp *Alw*NI/*Pvu*II fragment of pBR322 was inserted into the *Eco*RV site of this same vector to obtain pHH/BR-ΔRNAs2.9. The latter plasmid contained one complete origin and another origin lacking the promoters for RNAI and RNAII, in opposite orientations (see Figs. 4 and 5). In all these three plasmids, the distance between origins was approximately 2.9 kb. Fig. 5 shows the restriction maps corresponding to these plasmids.

Plasmid DNA was isolated from exponentially growing cells that had been transfected with each of these three new plasmids. The DNAs were digested with *Hin*dIII and independently analyzed by two-dimensional agarose gel electrophoresis. Fig. 6 shows the autoradiograms corresponding to pHH/BR-BR2.9, pHH/BR-Δpass2.9, and pHH/BR-ΔRNAs2.9. They were all hybridized with pBR322 DNA used as a probe.

In Fig. 6*A*, corresponding to pHH/BR-BR2.9 digested with *Hin*dIII (see Fig. 5), the lower diagonal arc corresponded to linear forms. The prominent spot at the *far right* end of the linear forms corresponded to the unreplicated linear form of the plasmid (1.0×). The continuous signal extending upward from the 1.0× linear form to the upper part of the autoradiogram corresponded to a bubble arc. A distinct spot, due to accumulated bubbles (5), was observed on top of the bubble arc. The small arc formed by a series of spots with decreasing intensity observed to the *right* of the accumulated bubbles extending downward corresponded to knotted bubbles (5). Two discrete double-Y signals were clearly visible to the left of the accumulated bubbles. Both signals emerged from the simple-Y arc (not visible in the autoradiogram) toward the signal of X-shaped recombinants. The relative mass of the molecules where the upper double-Y started was 1.6× the mass of the unreplicated linear form, whereas that one corresponding to the lower double-Y signal was 1.8×. As in all previous cases, the intensity of these double-Y signals became progressively stronger as they got closer to the X-shaped recombinants. Overall, the intensity of both signals was similar, indicating that in this particular plasmid initiation of DNA replication at oriα and oriβ occurred with a similar frequency.

Fig. 6*B* shows the autoradiogram corresponding to the two-dimensional agarose gel analysis of pHH/BR-Δpass2.9 digested with *Hin*dIII. The signals for accumulated bubbles and knotted bubbles were clearly visible. Surprisingly, however, only one termination signal was detected. It corresponded to an initiation event at oriα. This observation demonstrated that in this particular plasmid initiation of DNA replication occurred almost exclusively at the complete origin. Even more important was the observation that despite the fact initiation occurred rarely at oriβ, the replication forks that initiated at oriα stalled as they reached oriβ. This clearly indicated that the element or elements responsible for the polar pausing of replication forks were fully active even when oriβ lacked both pas sites.

Fig. 6*C* shows the autoradiogram corresponding to pHH/BR-ΔRNAs2.9 digested with *Hin*dIII. The complete bubble arc was obvious as well as the signal for accumulated bubbles. The latter, however, appeared less prominent than in the two previous cases. More importantly, no signal for knotted bubbles was observed. Besides, only one prominent termination signal was detected, although in this case it corresponded to the other origin, indicating preferential initiation of DNA replication at oriβ. This was the origin lacking the RNA promoters (see Figs. 4 and 5).

It has been reported that, in primer promoter deletions, the origin can presumably be primed by promoters located further upstream (21–23). In pHH/BR-ΔRNAs2.9, the origin lacking the RNA promoters had been inserted into the *Eco*RV restriction site of pBR322, interrupting the tetracycline resistance gene but without inactivating its promoter (see Figs. 4 and 5). Therefore, it was possible that the preferential initiation of DNA replication at oriβ in pHH/BR-ΔRNAs2.9 was driven by the constitutive promoter for the tetracycline resistance gene. To check this hypothesis, we deleted the 29-bp *Eco*RI-*Hin*dIII

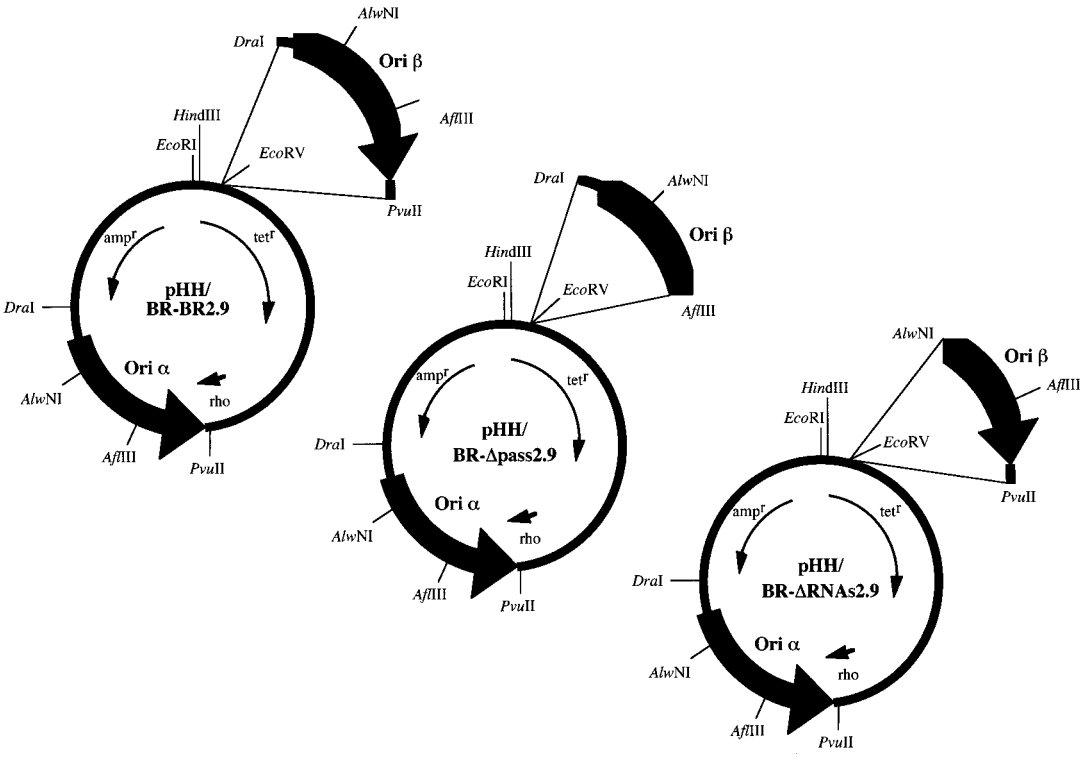

FIG. 5. **Construction strategy and restriction map of the plasmids derived from pBR322 containing two inversely oriented ColE1 origins.** The three restriction maps correspond to the circular plasmid pBR322. The *thick arrow* on the *circle* indicates the location and orientation of the complete origin (Oriα). The *thin arrows* within the *circle* indicate the location and transcription directions of the ampicillin and tetracycline resistance genes as well as rho. The places for a number of restriction endonucleases with a single recognition site are indicated. The *thick arrows* outside the pBR322 maps represent the three different fragments containing the inversely oriented origin (Oriβ) either complete (the *Dra*I-*Pvu*II fragment) or the partially deleted ones (the *Alw*NI-*Pvu*II fragment or the *Dra*I-*Afl*III fragment) that were cloned into the *Eco*RV site of pBR322. The names of the resulting plasmids are indicated. For details, see text.

fragment of pHH/BR-ΔRNAs2.9 containing the tetracycline resistance gene promoter and replaced it with the polylinker of pUC18. In this way we obtained a new plasmid named pHH/BR18-ΔRNAs2.9. It was almost identical to pHH/BR-ΔRNAs2.9, except that it lacked the promoter for the tetracycline resistance gene located upstream oriβ.

Fig. 6*D* shows the autoradiogram of the two-dimensional gel analysis corresponding to the RIs of pHH/BR18-ΔRNAs2.9 digested with *Hin*dIII. It was obvious that in this new plasmid initiation of DNA replication switched back to oriα. As in the previous case, however, no signal for knotted bubbles was detected even after longer exposures of the autoradiogram and the signal for accumulated bubbles was not as prominent as in pHH/BR-BR2.9 (Fig. 6*A*) or pHH/BR-Δpass2.9 (Fig. 6*B*). The speck above the signal for accumulated bubbles was a blotting artifact, and the faint signal below the bubble arc corresponded to broken bubbles (7, 12, 24, 25). This experiment demonstrated that in the absence of an upstream promoter, initiation at the origin lacking the RNA promoters was negligible. Pausing of the replication forks initiated at the other origin and formation of knotted bubbles were also significantly reduced.

Table I summarizes the results obtained for the last series of plasmids. It should be clearly pointed out, however, that throughout this study comparison of the relative intensities of specific products among different autoradiograms is not meant to be quantitative. In pHH/BR-BR2.9 (containing two complete origins), both origins appeared able to initiate replication as well as to stall replication forks initiated at the other origin. Both accumulated and knotted bubbles also were evident. In pHH/BR-Δpass2.9 (containing one complete origin (oriα) and another origin lacking the pas sites (oriβ)) initiation of DNA replication occurred primarily at the complete origin (oriα), although oriβ was still able to stall replication forks initiated at the other origin. Accumulated and knotted bubbles also were evident. In pHH/BR-ΔRNAs2.9 (containing one complete origin (oriα) and another origin lacking the RNA promoters (oriβ)) initiation occurred primarily at oriβ, the origin lacking the RNA promoters. No knotted bubbles were detected, and the signal for accumulated bubbles appeared significantly weaker than in the two previous cases. Finally, in pHH/BR18-ΔRNAs2.9 (containing one complete origin (oriα) and another origin lacking the RNA promoters (oriβ) where the upstream promoter for the tetracycline resistance gene had been deleted), initiation of DNA replication occurred almost exclusively at the complete origin (oriα). As in the previous case, however, no knotted bubbles were detected and the signal for accumulated bubbles was less conspicuous than in the first two cases.

These results, together with the observation that in all plasmids bearing two inversely oriented ColE1 origins only one origin fires per replication round as no termination signal can be detected along the region between origins (5), indicated that the presence of a transcription promoter upstream of the origin was the only essential requirement for it to stall other replicating forks traveling in the opposite direction. This observation strongly suggests that when a replication fork encounters the 3′ RNA end of an RNA-DNA hybrid, it pauses. The question is why. In *E. coli*, the DnaB protein is responsible for unwinding duplex DNA ahead of the replisome (26–28), and helicase inhibition is known to cause the arrest of replication forks (8, 9, 29, 30).

DnaB Helicase Is Unable to Dissociate RNA-DNA Hybrids—To test whether or not DnaB helicase was competent to dissociate DNA-DNA homoduplexes as well as RNA-DNA hybrids, two different substrates were constructed. To prepare the DNA-DNA homoduplex, a ^{32}P-end-labeled, 45-nucleotide oligonucleotide was partially annealed to a large ssDNA circle.

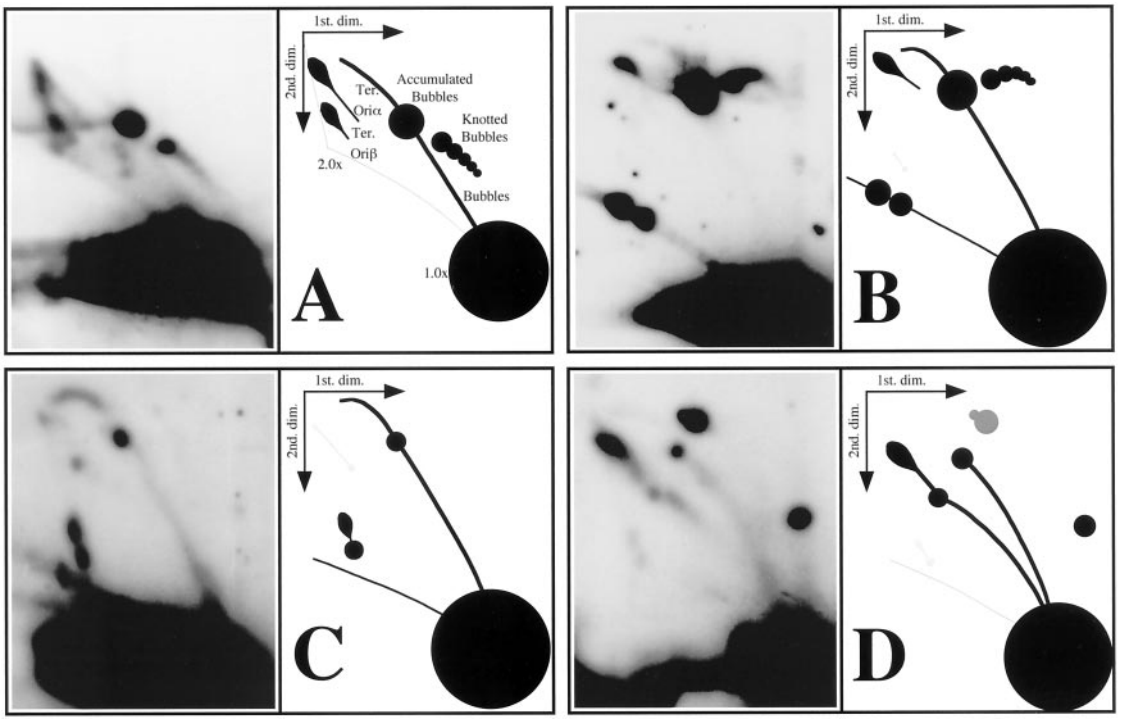

FIG. 6. **Two-dimensional agarose gel electrophoresis of the RIs corresponding to four different plasmids.** *A*, pHH/BR-BR2.9; *B*, pHH/BR-Δpass2.9; *C*, pHH/BR-ΔRNAs2.9; *D*, pHH/BR18-ΔRNAs2.9. All four plasmids were linearized with *Hin*dIII. The photographs of selected autoradiograms are shown to the *left* with a diagrammatic interpretation to the *right*. These diagrams were prepared after studying different exposures in order to confirm the nature of each signal. The names given throughout the text to the most prominent signals are depicted only for pHH/BR-BR2.9 (*A*).

TABLE I

Summary of the results obtained in the analysis of the replication mode of pBR322-derived plasmids containing two inversely oriented ColE1 origins

A schematic map of the most relevant structural elements involved are depicted in column 2. In pHH/BR-BR2.9, initiation occurred in both origins with similar efficiency. The signal for accumulated bubbles was prominent as well as the presence of knotted bubbles. In pHH/BR-Δpass2.9, initiation of DNA replication occurred mainly at Oriα. However, the signal for accumulated and knotted bubbles was as prominent as in pHH/BR-BR2.9. In pHH/BR-ΔRNAs2.9, initiation of DNA replication occured mainly at Oriβ. The strength of the signal for accumulated bubbles was significantly reduced compared with the two previous plasmids, and no knotted bubbles were detected. Finally, in pHH/BR18-ΔRNAs2.9, initiation of DNA replication switched back to Oriα. But as in pHH/BR-ΔRNAs2.9, the strength of the signal for accumulated bubbles was significantly reduced, and no knotted bubbles were detected.

Name	Map	Oriα	Oriβ	Acc. Bubbles	Knotted Bubbles
pHH/BR-BR2.9	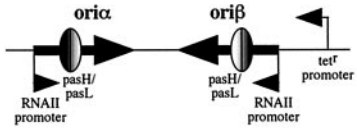	+++	+++	+++	+
pHH/BR-Δpass2.9	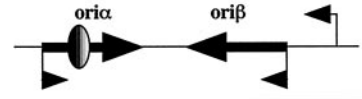	+++	+	+++	+
pHH/BR-ΔRNAs2.9	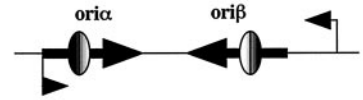	+	+++	+	
pHH/BR18-ΔRNAs2.9	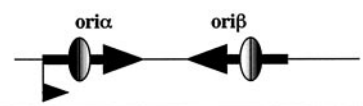	+++	+	+	

This oligonucleotide contained a 12-nucleotide-long tail that was not complementary to the DNA circle and remained free at its 3′ end. It was repeatedly shown that the efficiency of *E. coli* DnaB to unwind DNA-DNA duplexes increases significantly when the duplex contains a 3′ hanging tail (31). Nevertheless, other similar DNA-DNA constructs were prepared containing no 3′ hanging tail, where the duplex was 45 to ~400 nucleotides long (data not shown). On the other hand, to prepare the RNA-DNA hybrid, a ^{32}P-uridine-labeled, 51-nucleotide RNA was completely annealed to the same region of the ssDNA circle

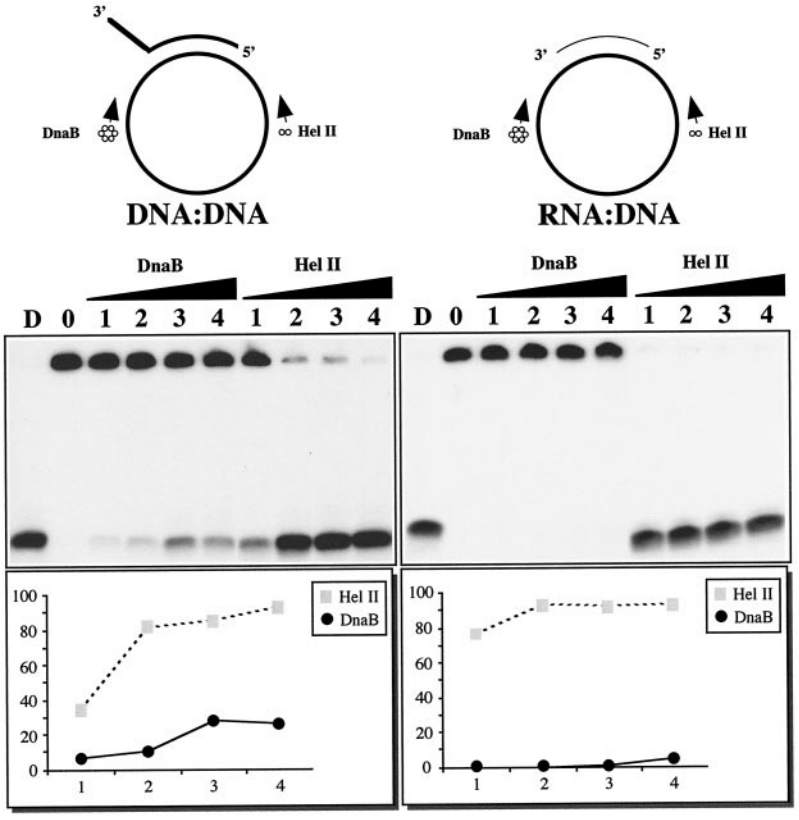

FIG. 7. ***In vitro* analysis of the ability of DnaB and helicase II of *E. coli* to unwind DNA-DNA homoduplexes and RNA-DNA hybrids.** A schematic representation of the helicase assay substrates is shown on *top*. The direction of DnaB and helicase II movement is indicated by an *arrow*. Autoradiograms of the polyacrylamide gels are shown in the *middle*. For the DNA-DNA homoduplex as well as for the RNA-DNA hybrid, 10 fmol of the substrate were used in each assay. *Lane D* corresponds to the substrate denatured by heat, *lane 0* corresponds to the untreated substrate, *lanes 1–4* correspond to the substrate incubated with 75, 150, 300, and 450 ng of DnaB or 3.7, 7.5, 15, and 30 ng of helicase II. The normalized densitometric analyses of both autoradiograms are shown below.

used before. This RNA-DNA substrate contains no 3′ hanging tail, since this is precisely the structure DnaB would encounter *in vivo* as the replicating fork advances toward the R-loop of an inversely oriented origin. Then, different amounts of *E. coli* DnaB and helicase II were tested for their ability to unwind the homoduplex as well as the hybrid *in vitro* and the products were analyzed by polyacrylamide gel electrophoresis. The autoradiograms and their corresponding phosphorimager densitometry are shown in Fig. 7. As shown previously by others, both helicases were able to dissociate the DNA-DNA homoduplex in a concentration-dependent manner, albeit helicase II was significantly more effective (9, 29, 32). Additionally, the ability of DnaB to unwind the DNA-DNA duplex was inversely proportional to the size of the duplex (Refs. 9, 29, and 32, and data not shown) and increases significantly when it contained a 3′ hanging tail (31). However, while helicase II was also able to dissociate the RNA-DNA hybrid, DnaB was clearly unable to do so.

Altogether these results strongly suggest that replication forks stall at silent ColE1 origins because the DnaB helicase is unable to unwind the RNA-DNA hybrid at the silent origin in a polar-dependent manner (Fig. 8).

DISCUSSION

One of our first goals was to find out whether or not two-dimensional agarose gel electrophoresis (6) could be used to determine the efficiency to initiate replication in non-palindromic plasmids containing two origins. A series of plasmids containing two ColE1 origins were constructed where both origins were in the same or in different orientations (Fig. 1). Taking advantage of the computer program designed by Viguera *et al.* (10), we predicted the shape of the RIs as well as the two-dimensional agarose gel patterns expected for different restriction fragments of these plasmids assuming that initiation occurred at only one of the origins per replication round (Fig. 2). The results obtained clearly indicated that two-dimensional agarose gel electrophoresis can be readily used to determine the efficiency to initiate replication for both origins in these plasmids (Fig. 3). The relative intensity of the termination signals reflected the efficiency of each origin to initiate replication.

The observation of prominent signals corresponding to accumulated and knotted bubbles (see Fig. 3) demonstrated that this peculiar replication behavior was not specific for *S. pyogens* pSM19035-derived plasmids (5), but is a general feature for all plasmids containing two inversely oriented ColE1 origins. The finding that pHT0.5, pHT2.0, and pHT5.8, all containing two ColE1 origins in the same orientation, showed neither accumulated nor knotted bubbles (Fig. 3*D* and data not shown) confirmed previous observations indicating the polar nature of this phenomenon (5, 7, 12, 34). The replication fork initiated at one origin stalled at the other silent origin only when both origins were inversely oriented.

The occurrence of several competent replication origins close to each other in a chromosome or in a plasmid creates a situation where replication initiates at only one of the closely spaced origins per replication round (7, 12–14, 35–37). This phenomenon was named origin interference (38). To find out if the physical distance between origins affected their capacity to interfere with each other and to act as a replication pausing site, we constructed a series of plasmids where the distance between origins varied from 0.5 to 5.8 kb (Fig. 1). No signal was detected, suggesting that both origins could be simultaneously active (Fig. 3). Moreover, the double-Y patterns observed in all three plasmids indicated that termination of DNA replication occurred at the same site where initiation took place, which is expected for plasmids that replicate in a unidirectional manner. These observations confirmed that only one origin was active per plasmid and replication round, although both origins were equally competent to initiate replication. Therefore, the interference between origins was operative in these plasmids

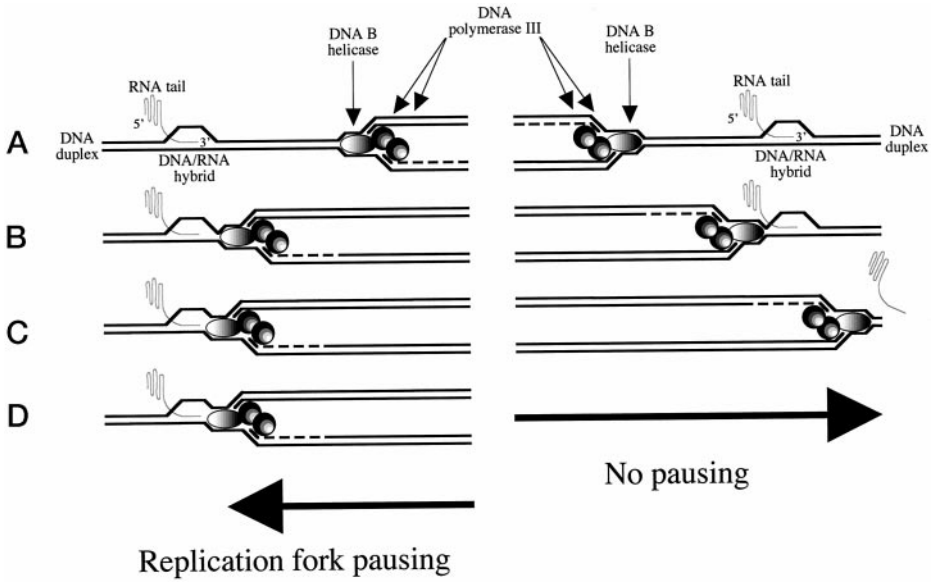

FIG. 8. **A model to explain the polar arrest of replication forks at silent ColE1 origins.** When the replisome, led by DnaB helicase, encounters the RNA 3′ end of the RNA-DNA hybrid at the silent origin, it would pause due to the inability of DnaB to unwind the hybrid. When the replisome approaches the hybrid from the other side, DnaB would find no obstacle as it moves in the 5′ to 3′ direction along the lagging strand template (67). This would explain why replication forks initiated at one origin pause at the other silent origin only if the origins are inversely oriented.

even when the distance between them increased up to 5.8 kb. The signals indicative for accumulated and knotted bubbles (5) were readily detected regardless of the distance separating the origins (see Fig. 3, *A–C*). This observation suggests that the element(s) responsible for the interference between origins and the stalling of replication forks in a polar-dependent manner reside(s) in the origin itself.

Several groups have clearly identified all the elements required for ColE1 origins to initiate replication (15–20). Fig. 4 highlights some of the most important events going on at ColE1 origins as initiation of DNA replication progresses. RNA polymerase initiates the transcription of RNAII from its promoter located 555 bp upstream the transition point between RNA and DNA, the point commonly regarded as the origin. As transcription progresses the RNAII transcript tail adopts a specific conformation that is prevented if another smaller transcript, RNAI (a 108-nucleotide-long molecule transcribed from the strand opposite to the one used to produce the RNAII primer), forms a complex with the RNAII tail. When the RNAII-DNA hybrid formation is stabilized, RNase H, specific for cleavage of the RNA in RNA-DNA hybrids, generates 3′-OH ends that serve as primers for DNA synthesis by DNA polymerase I (pol I). Finally, DNA polymerase III (pol III) replaces pol I 400 bp downstream of the origin at the primosome assembly site on the continuous strand template (pasH). The pas site on the discontinuous strand (pasL) is 150 bp downstream of the origin and functions in the primosome assembly on this strand (39). It is known, however, that the pas sites are not essential for ColE1 origins to initiate replication (40). Indeed, the ColE1 origin of the pUC vectors has the *lacZ* gene with the polylinker inserted between pasH and pasL; the minimal origin we used as oriβ in our pHH and pHT series lacked both pasH as well as pasL. Nevertheless, both origins initiated replication quite efficiently (Fig. 3).

To find out how efficient an origin lacking the RNA promoters or the pas sites is to initiate replication and to act as a pausing site compared with a complete origin, we constructed three new plasmids containing one complete origin (oriα) and another complete or partially deleted origin (oriβ). These plasmids were named pHH/BR-BR2.9, pHH/BR-Δpass2.9, and pHH/BR-ΔRNAs2.9. Both origins were equally competent to initiate replication in pHH/BR-BR2.9. In pHH/BR-Δpass2.9, however, initiation predominantly took place at oriα, indicating that the complete origin was more efficient than an origin lacking the pas sites to initiate replication. To our surprise, in pHH/BR-ΔRNAs2.9, initiation occurred basically at the origin lacking the RNA promoters. It has been reported that, in primer promoter deletions, the origin can presumably be primed by promoters located further upstream (21–23). To find out if the preferential initiation of DNA replication at oriβ we found in pHH/BR-ΔRNAs2.9 was driven by the constitutive promoter for the tetracycline resistance gene, we deleted this promoter and replaced it with the polylinker of pUC18. pHH/BR18-ΔRNAs2.9 was almost identical to pHH/BR-ΔRNAs2.9, except that it lacked the 29-bp *Eco*RI-*Hin*dIII fragment containing the promoter for the tetracycline resistance gene located upstream of oriβ. Fig. 6*D* shows that, in this new plasmid, initiation of DNA replication switched back to the complete origin. These observations demonstrated that when a plasmid was forced to choose between two origins to initiate replication, the complete origin was more efficient than an origin lacking either the pas sites or the RNA promoters in the absence of read-through transcription.

When compared for their efficiency to function as polar pausing sites, the origin lacking the pas sites proven to be as efficient as a complete origin. In pHH/BR-Δpass2.9, almost all plasmids initiated replication at oriα. But the signal for accumulated and knotted bubbles were still as strong as in pHH/BR-BR2.9. This observation indicated that the replication forks initiated at oriα stalled as they reached oriβ, which in this particular case, lacked the pas sites. In contrast, in pHH/BR18-ΔRNAs2.9 (see Fig. 6*D*), the signal for accumulated bubbles was less conspicuous than in the first two cases. Moreover, no signal for knotted bubbles was detected. These observations indicated that an origin lacking the RNA promoters (or other potential promoters upstream of the origin) is less competent to stall replication forks moving in the opposite direction. Altogether, this means that transcription and the subsequent formation of a stable RNA-DNA hybrid was the only requirement for a silent origin to block replication forks in a polar fashion.

The result obtained with pHH/BR-ΔRNAs2.9 deserves special comment. In this plasmid, almost all the initiation events occurred at oriβ, the origin lacking the RNA promoters. Priming was driven by the tetracycline resistance gene promoter, as demonstrated by the switch in initiation to oriα when this promoter was deleted (see Fig. 6*D*). However, the replication forks initiated at oriβ did not pause at oriα (the complete origin in this plasmid) as in pHH/BR-BR2.9 or pHH/BR-Δpass2.9 (note the absence of knotted bubbles and the intensity of the signal for accumulated bubbles in Fig. 6, panel *C* compared

with panels *A* and *B*). A plausible explanation for this difference is that the ColE1 copy number control mechanism was responsible for the unstableness of RNAII/DNA hybrids at oriα. Formation of this hybrid is essential for priming DNA replication (see Fig. 4). RNAI, by complexing with RNAII, blocks its folding into the conformation required to form a stable hybrid. For this reason, RNAI is often referred to as a trans-acting regulator of ColE1 replication (39). In pHH/BR-ΔRNAs2.9, the only target for RNAI occurred at oriα. The other origin, oriβ, lacked the *Dra*I-*Alw*NI fragment (see Fig. 4). This is the control region upstream of the origin where the "kissing" interaction between RNAI and RNAII takes place (39). Those replication forks initiated at oriβ would encounter no stable RNAII/DNA hybrid at oriα and would not stall. The high efficiency of the constitutive tetracycline resistance promoter and the absence of the copy number control region upstream oriβ could explain both the high efficiency of oriβ to initiate replication as well as the inability of oriα to stall replication forks initiated at oriβ.

What may cause a replication fork to stop at a silent origin in a polar-dependent manner? One of the best characterized replication fork barriers (RFBs) occurs in the bi-directionally replicated circular chromosome of *E. coli* (30, 41). The region where replication forks meet, about 180° opposite the origin, is flanked by several polar RFBs. These RFBs are arranged in such a way to form a termination trap. These barriers, named Ter sites, are 23-bp-long sequences that recognize and bind a protein named Tus (42). The Ter-Tus complex arrests progression of replication forks by inhibiting the unwinding reaction catalyzed by DnaB helicase in an orientation-dependent manner (8, 9, 29).

Head-on collision between replication and transcription appears to be deleterious and is specifically avoided in the genomes of many prokaryotes and eukaryotic organisms (9, 43–47). In higher eukaryotes, a conserved specific RFB was found close to the 3′ end of the rRNA transcription unit (48–55). It was speculated that the main function of this barrier would be to prevent collision between replication and transcription (50, 56). In *Saccharomyces cerevisiae*, however, it was repeatedly shown that transcription itself is not responsible for the pausing of replication forks at the 3′ end of the rRNA transcription unit (56, 57). Whether or not co-directional collisions also cause DNA replication arrest is still a matter of controversy (58, 59). Stalling of replication forks due to the specific DNA binding of a protein or protein complexes has been reported also for OriP in the Epstein-Barr virus (60–62) and for centromeric DNA sequences in *S. cerevisiae* (63). Finally, experimental evidence indicates that replication forks also pause at $(dG\text{-}dA)_n$-(dT-dC)n tracts (64, 65) and trinucleotide repeats (66) *in vivo*.

As previously mentioned, in *E. coli* the DnaB protein is the primary replicative helicase responsible for unwinding duplex DNA ahead of the replisome (26–28). *In vitro* replication assays showed that DnaB unwinds duplex DNA moving in the 5′ to 3′ direction along the lagging strand template (67). The unwinding reaction catalyzed by DnaB is favored by the presence of a 3′ single-stranded tail on the DNA to be displaced (31). For this reason we made the two substrates different, to reflect the situation *in vivo*. However, the same result was obtained when the DNA-DNA and the RNA-DNA substrates had the same structure (data not shown). The observation that Ter-Tus complexes arrest progression of replication forks by inhibiting the unwinding reaction catalyzed by DnaB (8) prompted the finding that other proteins bound to specific DNA sequences can also inhibit DnaB. It was shown that bound Lac repressor protein also inhibits the unwinding catalyzed by DnaB, whereas helicase II, another *E. coli* helicase, is perfectly able to displace this protein from duplex DNA (68). Helicase II is one of the very few helicases that can unwind RNA-DNA hybrids *in vitro* (33), although the significance for this role in nucleic acids metabolism is still unclear.

The observations made in the course of this study led us to speculate that initiation of DNA replication at ColE1 origins is a two-step process. Synthesis of the RNA primer by RNA polymerase and stabilization of the hybrid appears to be constitutive, as they take place even when the origin remains silent. The second step, elongation of the primer and assembly of the primosome, may or may not follow but is regulated by different and still unknown factors. We showed also that DnaB is not able to unwind RNA-DNA hybrids *in vitro* (see Fig. 7). During initiation of DNA replication at ColE1 origins, following formation of a stable RNAII-DNA hybrid, RNase H cleaves the RNA of the hybrid, generating 3′-OH ends that serve as primers for DNA synthesis by pol I (69). If pol I fails to elongate the primer, another replication fork coming in the opposite direction would directly meet the hybrid. DnaB, being unable to dissociate this structure, would be the ultimate responsible for the polar stalling of replication forks precisely at the origin (see Fig. 8). Alternatively, it could be that even at the silent origin pol I is able to extend the RNA II primer to form a *bonna fide* replication fork. This fork, however, would not be able to progress more than a few nucleotides as pausing always occurs very close to the origin and no termination signal could be detected along the region between the origins (5).

Acknowledgments—We are grateful to Bidyut Mohanty, Enrique Viguera, Alicia Sánchez, Natasha Vanegas, and Leticia Olavarrieta for discussions and suggestions during the course of this study; to P. Robles for technical assistance; to Deepak Bastia for kindly providing us with helicase II and the overproducer for DnaB; and to Ramón Díaz-Orejas for critical reading of the manuscript.

REFERENCES

1. Collins, J. (1981) *Cold Spring Harbor Symp. Quant. Biol.* **45,** 409–416
2. Mizuuchi, K., Mizuuchi, M., and Gellert, M. (1982) *J. Mol. Biol.* **156,** 229–243
3. Ceglowski, P., Lurz, R., and Alonso, J. C. (1993) *FEMS Microbiol. Lett.* **109,** 145–150
4. Ceglowski, P., and Alonso, J. C. (1994) *Gene* (*Amst.*) **145,** 33–39
5. Viguera, E., Hernandez, P., Krimer, D. B., Boistov, A. S., Lurz, R., Alonso, J. C., and Schvartzman, J. B. (1996) *J. Biol. Chem.* **271,** 22414–22421
6. Brewer, B. J., and Fangman, W. L. (1987) *Cell* **51,** 463–471
7. Martín-Parras, L., Hernández, P., Martínez-Robles, M. L., and Schvartzman, J. B. (1992) *J. Biol. Chem.* **267,** 22496–22505
8. Khatri, G. S., MacAllister, T., Sista, P. R., and Bastia, D. (1989) *Cell* **59,** 667–674
9. Sahoo, T., Mohanty, B. K., Lobert, M., Manna, A. C., and Bastia, D. (1995) *J. Biol. Chem.* **270,** 29138–29144
10. Viguera, E., Rodríguez, A., Hernández, P., Krimer, D. B., Trelles, O., and Schvartzman, J. B. (1998) *Gene* (*Amst.*) **217,** 41–49
11. Friedman, K. L., and Brewer, B. J. (1995) in *DNA Replication* (Campbell, J. L., ed) Vol. 262, pp. 613–627, Academic Press Inc., San Diego
12. Martín-Parras, L., Hernández, P., Martínez-Robles, M. L., and Schvartzman, J. B. (1991) *J. Mol. Biol.* **220,** 843–853
13. Schvartzman, J. B., Adolph, S., Martín-Parras, L., and Schildkraut, C. L. (1990) *Mol. Cell. Biol.* **10,** 3078–3086
14. Liu, Y., and Botchan, M. (1990) *J. Virol.* **64,** 5903–5911
15. Marians, K. J. (1992) *Annu. Rev. Biochem.* **61,** 673–719
16. Dasgupta, S., Masukata, H., and Tomizawa, J. (1987) *Cell* **51,** 1113–1122
17. Minden, J. S., and Marians, K. J. (1985) *J. Biol. Chem.* **260,** 9316–9325
18. Nakasu, S., and Tomizawa, J. (1992) *Proc. Natl. Acad. Sci. U. S. A.* **89,** 10139–10143
19. Tomizawa, J., Sakakibara, Y., and Kakefuda, T. (1974) *Proc. Natl. Acad. Sci. U. S. A.* **71,** 2260–2264
20. Inselburg, J. (1974) *Proc. Natl. Acad. Sci. U. S. A.* **71,** 2256–2259
21. Oka, A., Nomura, N., Morita, M., Sugisaki, H., Sugimoto, K., and Takanami, M. (1979) *Mol. Gen. Genet.* **172,** 151–159
22. Cesareni, G. (1982) *J. Mol. Biol.* **160,** 123–126
23. Panayotatos, N. (1984) *Nucleic Acids Res.* **12,** 2641–2648
24. Kalejta, R. F., and Hamlin, J. L. (1996) *Mol. Cell. Biol.* **16,** 4915–4922
25. Linskens, M. H. K., and Huberman, J. A. (1990) *Nucleic Acids Res.* **18,** 647–652
26. West, S. W. (1996) *Cell* **86,** 177–180
27. Baker, T. A., and Bell, S. P. (1998) *Cell* **92,** 295–305
28. Stillman, B. (1996) in *DNA Replication in Eukaryotic Cells* (DePamphilis, M. L., ed) pp. 435–460, Cold Spring Harbor Laboratory Press, Cold Spring Harbor, NY
29. Sahoo, T., Mohanty, B. K., Patel, I., and Bastia, D. (1995) *EMBO J.* **14,** 619–628
30. Bastia, D., and Mohanty, B. K. (1996) in *DNA Replication in Eukaryotic Cells* (DePamphilis, M. L., ed) pp. 177–215, Cold Spring Harbor Laboratory

Press, Cold Spring Harbor, NY
31. LeBowitz, J. H., and McMacken, R. (1986) *J. Biol. Chem.* **261,** 4738–4748
32. Mohanty, B. K., Sahoo, T., and Bastia, D. (1996) *EMBO J.* **15,** 2530–2539
33. Matson, S. W. (1989) *Proc. Natl. Acad. Sci. U. S. A.* **86,** 4430–4434
34. Schvartzman, J. B., Martínez-Robles, M. L., and Hernández, P. (1993) *Nucleic Acids Res.* **21,** 5474–5479
35. Brewer, B. J., and Fangman, W. L. (1993) *Science* **262,** 1728–1731
36. Brewer, B. J., and Fangman, W. L. (1994) *Proc. Natl. Acad. Sci. U. S. A.* **91,** 3418–3422
37. Marahrens, Y., and Stillman, B. (1994) *EMBO J.* **13,** 3395–3400
38. Newlon, C. S. (1996) in *DNA Replication in Eukaryotic Cells* (DePamphilis, M. L., ed) pp. 873–914, Cold Spring Harbor Laboratory Press, Cold Spring Harbor, NY
39. Kornberg, A., and Baker, T. A. (1992) *DNA Replication*, 2nd Ed., W. H. Freeman and Co., New York
40. Van der Ende, A., Teertstra, R., and Weisbeek, P. J. (1983) *J. Mol. Biol.* **167,** 751–756
41. Hill, T. M., Pelletier, A. J., Tecklenburg, M. L., and Kuempel, P. L. (1988) *Cell* **55,** 459–466
42. Kuempel, P. L., Pelletier, A. J., and Hill, T. M. (1989) *Cell* **59,** 581–583
43. Brewer, B. J. (1988) *Cell* **53,** 679–686
44. Liu, B., and Alberts, B. M. (1995) *Science* **267,** 1131–1137
45. French, S. (1992) *Science* **258,** 1362–1365
46. Deshpande, A. M., and Newlon, C. S. (1996) *Science* **272,** 1030–1033
47. Mohanty, B. K., Sahoo, T., and Bastia, D. (1998) *J. Biol. Chem.* **273,** 3051–3059
48. Brewer, B. J., and Fangman, W. L. (1988) *Cell* **55,** 637–643
49. Linskens, M. H. K., and Huberman, J. A. (1988) *Mol. Cell. Biol.* **8,** 4927–4935
50. Hernández, P., Martín-Parras, L., Martínez-Robles, M. L., and Schvartzman, J. B. (1993) *EMBO J.* **12,** 1475–1485
51. Wiesendanger, B., Lucchini, R., Koller, T., and Sogo, J. M. (1994) *Nucleic Acids Res.* **22,** 5038–5046
52. Little, R. D., Platt, T. H. K., and Schildkraut, C. L. (1993) *Mol. Cell. Biol.* **13,** 6600–6613
53. López-Estraño, C., Schvartzman, J. B., and Hernández, P. (1997) *Chromosomes Today* **12,** 149–169
54. López-Estraño, C., Schvartzman, J. B., Krimer, D. B., and Hernández, P. (1998) *J. Mol. Biol.* **277,** 249–256
55. Gerber, J. K., Gogel, E., Berger, C., Wallisch, M., Muller, F., Grummt, I., and Grummt, F. (1997) *Cell* **90,** 559–567
56. Brewer, B. J., Lockshon, D., and Fangman, W. L. (1992) *Cell* **71,** 267–276
57. Kobayashi, T., Hidaka, M., Nishizawa, M., and Horiuchi, T. (1992) *Mol. Gen. Genet.* **233,** 355–362
58. Liu, B., Wong, M. L., Tinker, R. L., Geiduschek, E. P., and Alberts, B. M. (1993) *Nature* **366,** 33–39
59. Elias-Arnanz, M., and Salas, M. (1997) *EMBO J.* **16,** 5775–5783
60. Gahn, T. A., and Schildkraut, C. L. (1989) *Cell* **58,** 527–535
61. Dhar, V., and Schildkraut, C. L. (1991) *Mol. Cell. Biol.* **11,** 6268–6278
62. Ermakova, O. V., Frappier, L., and Schildkraut, C. L. (1996) *J. Biol. Chem.* **271,** 33009–33017
63. Greenfeder, S. A., and Newlon, C. S. (1992) *Mol. Cell. Biol.* **12,** 4056–4066
64. Rao, B. S. (1994) *Gene* (*Amst.*) **140,** 233–237
65. Peleg, M., Kopel, V., Borowiec, J. A., and Manor, H. (1995) *Nucleic Acids Res.* **23,** 1292–1299
66. Samadashwily, G. M., Raca, G., and Mirkin, S. M. (1997) *Nat. Genet.* **17,** 298–304
67. Matson, S. W., Bean, D. W., and George, J. W. (1994) *Bioessays* **16,** 13–22
68. Yancey-Wrona, J. E., and Matson, S. W. (1992) *Nucleic Acids Res.* **20,** 6713–6721
69. Itoh, T., and Tomizawa, J. (1980) *Proc. Natl. Acad. Sci. U. S. A.* **77,** 2450–2454

DnaB Helicase Is Unable to Dissociate RNA-DNA Hybrids: ITS IMPLICATION IN THE POLAR PAUSING OF REPLICATION FORKS AT ColE1 ORIGINS

David Santamari?a, Guillermo de la Cueva, Mari?a Luisa Marti?nez-Robles, Dora B. Krimer, Pablo Hernández and Jorge B. Schvartzman

J. Biol. Chem. 1998, 273:33386-33396.
doi: 10.1074/jbc.273.50.33386